Inorganic Chemistry

ARTICLE

pubs.acs.org/IC

Syntheses, Structures, and Magnetic Properties of Low-Dimensional Heterometallic Complexes Based on the Versatile Building Block $[(Tp)Cr(CN)_3]^-$

Min-Xia Yao,[†] Zheng-You Wei,[†] Zhi-Guo Gu,[†] Qi Zheng,[†] Yan Xu,[‡] and Jing-Lin Zuo*[,†]

[†]State Key Laboratory of Coordination Chemistry, School of Chemistry and Chemical Engineering, Nanjing National Laboratory of Microstructures, Nanjing University, Nanjing 210093, P. R. China

[‡]State Key Laboratory of Materials-Oriented Chemical Engineering, College of Chemistry and Chemical Engineering, Nanjing University of Technology, Nanjing 210009, P. R. China

Supporting Information

ABSTRACT: Using the tricyano precursor $(Bu_4N)[(Tp)Cr(CN)_3]$ (Bu_4N^+ = tetrabutylammonium cation; Tp = tris(pyrazolyl)hydroborate), a pentanuclear heterometallic cluster $[(Tp)_2Cr_2(CN)_6Cu_3(Me_3tacn)_3][(Tp)Cr(CN)_3](ClO_4)_3\cdot 5H_2O$ (**1**, Me_3tacn = *N*,*N*′,*N*″-trimethyl-1,4,7-triazacyclononane), three tetranuclear heterometallic clusters $[(Tp)_2Cr_2(CN)_6Cu_2(L_{OEt})_2]\cdot 2.5CH_3CN$ (**2**, L_{OEt} = $[(Cp)Co(P(O)(OEt)_2)_3]$, Cp = cyclopentadiene), $[(Tp)_2Cr_2(CN)_6Mn_2(L_{OEt})_2]\cdot 4H_2O$ (**3**), and $[(Tp)_2Cr_2(CN)_6Mn_2(phen)_4](ClO_4)_2$ (**4**, phen = phenanthroline), and a one-dimensional (1D) chain polymer $[(Tp)_2Cr_2(CN)_6Mn(bpy)]_n$ (**5**, bpy = 2,2′-bipyridine) have been synthesized and structurally characterized. Complex **1** shows a trigonal bipyramidal geometry in which $[(Tp)Cr(CN)_3]^-$ units occupy the apical positions and are linked through cyanide to $[Cu(Me_3tacn)]^{2+}$ units situated in the equatorial plane. Complexes **2**−**4** show similar square structures, where Cr^{III} and M^{II} ($M = Cu^{II}$ or Mn^{II}) ions are alternatively located on the rectangle corners. Complex **5** consists of a 4,2-ribbon-like bimetallic chain. Ferromagnetic interactions between Cr^{III} and Cu^{II} ions bridged by cyanides are observed in complexes **1** and **2**. Antiferromagnetic interactions are presented between Cr^{III} and Mn^{II} ions bridged by cyanides in complexes **3**−**5**. Complex **5** shows metamagnetic behavior with a critical field of about 22.5 kOe at 1.8 K.

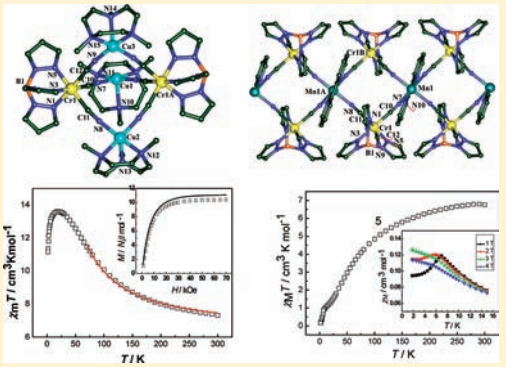

INTRODUCTION

Since the discovery of the first single-molecule magnet (SMM), $[Mn_{12}O_{12}(MeCO_2)_{16}(H_2O)_4]$, numerous other molecules with similar SMMs behavior have been studied. To date, the majority of them are transition-metal−oxo clusters.[1] Cyanide, as a short and conjugated linear ligand being able to mediate the magnetic interaction between two metal ions,[2] is an alternative bridging ligand for preparing high-spin clusters. Thus far, many cyanometalate compounds have been reported, and they show a variety of magnetism, including room-temperature magnets, spin-crossover materials, single-molecule magnets (SMMs), single-chain magnets (SCMs), photomagnetism, and magneto-optics.[3]

One effective method to prepare cyanometalate clusters with predictable and tunable properties refers to the employment of modified hexacyanometalates or octacyanometalates $[(L)M(CN)_q]^{p-}$ units (where L = polydentate N-donor or P-donor chelating ligands; M = V, Cr, Fe, Mo, W, Re, etc.) as building blocks toward fully solvated transition-metal ions or coordinatively unsaturated metal complexes.[4−9] $[(L_{Tp})Fe(CN)_3]^-$ (Scheme 1) are typical examples of the building blocks and widely studied in our group because of the virtue of good solubility and the low-spin Fe^{III} ion possessing obvious single-ion magnetic anisotropy.[10] With the use of these magnetic anisotropic precursors, some interesting cyano-bridged complexes have been successfully obtained.[2f,11−13]

As part of a continual effort to develop new examples of cyano-bridged heterobimetallic magnetic complexes, we chose another tricyanometalate precursor, $[(Tp)Cr(CN)_3]^-$, first reported by Long's group,[5b] to synthesize new low-dimensional cyano-bridged magnetic compounds. Aside from the virtue of good solubility, the chromium(III) ion in $[(Tp)Cr(CN)_3]^-$ has three unpaired electrons against only one in the case of the related low-spin iron(III) derivatives. Thus, substituting Cr^{III} for Fe^{III} is an effective means of increasing the strength of the magnetic exchange coupling.[14,15]

In this paper, Kläui's tripodal ligand, $[(Cp)Co(P(O)(OEt)_2)_3]^-$ (L_{OEt}), is used as an auxiliary ligand. Compared with organic ligands of σ-electron donors, such as phenanthroline and 2,2′-bipyridine, this oxygen-containing tripodal ligand possesses large steric hindrance and good π-electron-donating ability. It is well known that the interactions between the

Received: June 2, 2011
Published: August 10, 2011

   dx.doi.org/10.1021/ic2011875 | *Inorg. Chem.* 2011, 50, 8636–8644

Scheme 1

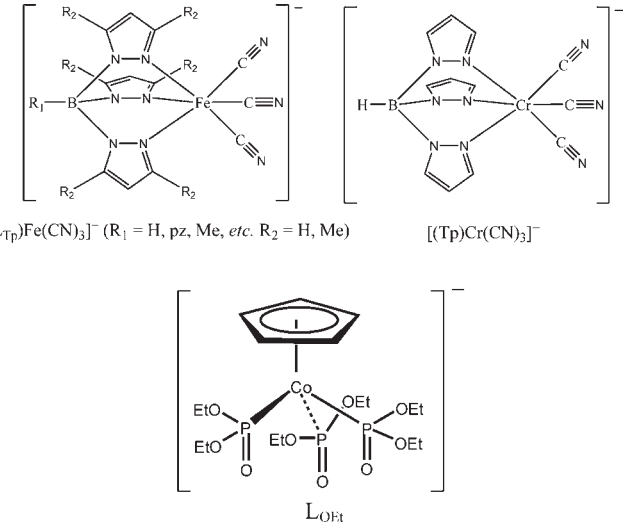

paramagnetic metal centers and the ligands affect the local electron structures of the metal ions,[16] which may influence the magnetic interaction between metal ions.

With these strategies in mind, five cyano-bridged compounds based on $[(Tp)Cr(CN)_3]^-$, a pentanuclear heterometallic cluster $[(Tp)_2Cr_2(CN)_6Cu_3(Me_3tacn)_3][(Tp)Cr(CN)_3](ClO_4)_3\cdot 5H_2O$ (**1**, Me_3tacn = *N*,*N*′,*N*′-trimethyl-1,4,7-triazacyclononane), three tetranuclear heterometallic clusters $[(Tp)_2Cr_2(CN)_6Cu_2(L_{OEt})_2]\cdot 2.5CH_3CN$ (**2**), $[(Tp)_2Cr_2(CN)_6Mn_2(L_{OEt})_2]\cdot 4H_2O$ (**3**), and $[(Tp)_2Cr_2(CN)_6Mn_2(phen)_4](ClO_4)_2$ (**4**, phen = phenanthroline), and a one-dimensional chain polymer $[(Tp)_2Cr_2(CN)_6Mn(bpy)]_n$ (**5**, bpy = 2,2′-bipyridine), were synthesized. Their crystal structures and magnetic properties were investigated.

EXPERIMENTAL SECTION

Starting Materials. $Na[(Cp)Co(P(O)(OEt)_2)_3]$ (NaL_{OEt}) and $(n\text{-}Bu_4N)[(Tp)Cr(CN)_3]$ were prepared according to the literature.[17,5b] Other materials were commercially available and used as received.

Caution: Although no problems were encountered in this work, perchlorate salts are potentially explosive and cyanides are very toxic. Thus, these starting materials should be handled in small quantities and with great care.

Preparation of $[(Tp)_2Cr_2(CN)_6Cu_3(Me_3tacn)_3][(Tp)Cr(CN)_3](ClO_4)_3\cdot 5H_2O$ (1). Solid $Cu(ClO_4)_2\cdot 6H_2O$ (14 mg, 0.04 mmol) and Me_3tacn (7.0 mg, 0.04 mmol) were mixed in 16 mL of dichloromethane and methanol (v/v = 3:1). Treatment of this mixture with $(n\text{-}Bu_4N)[(Tp)Cr(CN)_3]$ (24 mg, 0.04 mmol) afforded a purple-red solution, which was magnetically stirred for 10 min and then filtered. Purple block-shaped crystals of **1** were obtained by filtration after slow evaporation of the resulting solution for several days. Yield: 48%. Anal. Calcd for $C_{63}H_{103}B_3Cl_3Cr_3Cu_3N_{36}O_{17}$: C, 35.66; H, 4.89; N, 23.76. Found: C, 35.68; H, 4.85; N, 23.75. IR (KBr, cm^{-1}): 2168 (ν_{CN}).

Preparation of $[(Tp)_2Cr_2(CN)_6Cu_2(L_{OEt})_2]\cdot 2.5CH_3CN$ (2). $Cu(ClO_4)_2\cdot 6H_2O$ (15 mg, 0.04 mmol) and NaL_{OEt} (23 mg, 0.04 mmol) were mixed in 8 mL of MeCN/EtOH (v/v = 2:1). Treatment of this mixture with $(n\text{-}Bu_4N)[(Tp)Cr(CN)_3]$ (24 mg, 0.04 mmol) afforded a green solution, which was magnetically stirred for 10 min and then filtered. Green block-shaped crystals were collected by filtration after slow evaporation of the resulting solution for several days. Yield: 76%. Anal. Calcd for $C_{63}H_{87.5}B_2Co_2Cr_2Cu_2N_{20.5}O_{18}P_6$: C, 38.29; H, 4.46; N, 14.53. Found: C, 38.40; H, 4.42; N, 14.54. IR (KBr, cm^{-1}): 2174 (ν_{CN}).

Preparation of $[(Tp)_2Cr_2(CN)_6Mn_2(L_{OEt})_2]\cdot 4H_2O$ (3). $Mn(ClO_4)_2\cdot 6H_2O$ (14 mg, 0.04 mmol) and NaL_{OEt} (23 mg, 0.04 mmol) were mixed in 16 mL of dichloromethane and methanol (v/v = 3:1). Treatment of this mixture with $(n\text{-}Bu_4N)[(Tp)Cr(CN)_3]$ (24 mg, 0.04 mmol) afforded a yellow solution, which was magnetically stirred for 10 min and then filtered. Yellow block-shaped crystals were collected by filtration after slow evaporation of the resulting solution for several days. Yield: 56%. Anal. Calcd for $C_{58}H_{98}B_2Co_2Cr_2Mn_2N_{18}O_{28}P_6$: C, 34.23; H, 4.85; N, 12.39. Found: C, 34.20; H, 4.81; N, 12.44. IR (KBr, cm^{-1}): 2223, 2158 (ν_{CN}).

Preparation of $[(Tp)_2Cr_2(CN)_6Mn_2(phen)_4](ClO_4)_2$ (4). Complex **4** as yellow block-shaped crystals was obtained by following the same procedure as described for complex **3** except phen was used instead of NaL_{OEt}. Yield: 79%. Anal. Calcd for $C_{72}H_{52}B_2Cl_2Cr_2Mn_2N_{26}O_8$: C, 50.40; H, 3.05; N, 21.23. Found: C, 50.42; H, 3.02; N, 21.20. IR (KBr, cm^{-1}): 2144 (ν_{CN}).

Preparation of $[(Tp)_2Cr_2(CN)_6Mn(bpy)]_n$ (5). Complex **5** as yellow rhombic crystals was obtained by following the same procedure as described for complex **3** except bpy was used instead of NaL_{OEt}. Yield: 61%. Anal. Calcd for $C_{34}H_{28}B_2Cr_2MnN_{20}$: C, 45.51; H, 3.15; N, 31.22. Found: C, 45.50; H, 3.13; N, 31.25. IR (KBr, cm^{-1}): 2137, 2158, and 2215 (ν_{CN}).

X-ray Structure Determination. Crystal structures were determined on a Siemens (Bruker) SMART CCD diffractometer using monochromated Mo Kα radiation (λ = 0.71073 Å) at 296 K for complexes **1**−**4** and 273 K for complex **5**. Cell parameters were retrieved using SMART software and refined using SAINT[18] on all observed reflections. Data was collected using a narrow-frame method with scan widths of 0.30° in ω and an exposure time of 10 s/frame. The highly redundant data sets were reduced using SAINT[18] and corrected for Lorentz and polarization effects. Absorption corrections were applied using SADABS[19] supplied by Bruker. Structures were solved by direct methods using the program SHELXL-97.[20] The positions of the metal atoms and their first coordination spheres were located from direct-methods *E* maps; other non-hydrogen atoms were found in alternating difference Fourier syntheses and least-squares refinement cycles and, during the final cycles, refined anisotropically. Hydrogen atoms were placed in calculated positions and refined as riding atoms with a uniform value of U_{iso} which are tied 1.2 times or 1.5 times (for methyl group) to the parent atoms. Final crystallographic data and values of R_1 and wR_2 are listed in Table 1. Selected bond distances and angles for complexes **1**−**5** are listed in Tables 2−5 and S1, Supporting Information.

Physical Measurements. Elemental analyses for C, H, and N were performed on a Perkin-Elmer 240C analyzer. Infrared spectra were recorded on a Vector22 Bruker Spectrophotometer with KBr pellets in the 400−4000 cm^{-1} region. Magnetic susceptibilities for all polycrystalline samples were measured with the use of a Quantum Design MPMS-XL7 SQUID magnetometer in the temperature range 1.8−300 K for complexes **1**−**3** and **5** and 2.0−300 K for complex **4**. Field dependences of magnetization were measured in an applied field up to 70 kOe for complexes **1**−**3** and **5** and 50 kOe for complex **4**. The ac magnetic susceptibility measurements were performed at various frequencies from 1 to 1500 Hz with the ac field amplitude of 5 Oe and no dc field applied.

RESULTS AND DISCUSSION

Crystal Structures. Complexes **1**−**5** are all air stable at room temperature, as evidenced by IR and UV−vis spectroscopic studies (see Figure S1, Supporting Information). No reorientation of cyanide ligands is observed for them.[5b,21]

Complex **1** consists of a cationic trigonal bipyramidal unit, $[(Tp)_2Cr_2(CN)_6Cu_3(Me_3tacn)_3]^{4+}$, one $[(Tp)Cr(CN)_3]^-$ anion, and three ClO_4^- anions. It is similar to $[Tp_2(Me_3tacn)_3Cu_3Fe_2(CN)_6](ClO_4)_4\cdot 2H_2O$ and $[(Me_3tacn)_5Cu_3Cr_2(CN)_6](ClO_4)_6\cdot 5CH_3CN$.[12a,21] As shown in Figure 1, the cluster has a

dx.doi.org/10.1021/ic2011875 |*Inorg. Chem.* 2011, 50, 8636–8644

Table 1. Summary of Crystallographic Data for Complexes 1−5[a]

	1	2	3	4	5
formula	$C_{63}H_{103}B_3Cl_3Cr_3Cu_3N_{36}O_{17}$	$C_{63}H_{87.5}B_2Co_2Cr_2Cu_2N_{20.5}O_{18}P_6$	$C_{58}H_{98}B_2Co_2Cr_2Mn_2N_{18}O_{28}P_6$	$C_{72}H_{52}B_2Cl_2Cr_2Mn_2N_{26}O_8$	$C_{34}H_{28}B_2Cr_2MnN_{20}$
fw	2122.21	1974.40	2034.70	1713.78	897.32
cryst syst	trigonal	monoclinic	triclinic	triclinic	monoclinic
space group	*R*3*m*	*C*2/*c*	$P\bar{1}$	$P\bar{1}$	*C*2/*c*
a, Å	34.6504(9)	33.292(3)	12.1232(16)	12.9684(10)	29.513(2)
b, Å	34.6504(9)	11.8118(11)	13.0166(17)	12.9945(11)	9.1437(7)
c, Å	23.2241(12)	25.210(2)	16.571(2)	13.6671(11)	14.7447(11)
a, deg	90	90	76.956(2)	65.8320(10)	90
β, deg	90	106.011(1)	70.039(2)	70.4820(10)	100.939(1)
γ, deg	120	90	75.755(2)	67.1830(10)	90
V, Å^3	24148.3(15)	9529.0(16)	2353.2(5)	1894.3(3)	3906.6(5)
Z	9	4	1	1	4
D_{calcd}, g cm^{-3}	1.313	1.376	1.434	1.502	1.526
T/K	296(2)	296(2)	296(2)	296(2)	273(2)
μ, mm^{-1}	1.020	1.166	1.006	0.750	0.921
θ, deg	1.11−26.00	1.27−26.00	1.66−26.00	1.67−25.21	1.41−25.50
F(000)	9846	4044	2400	870	1820
index ranges	$-42 \le h \le 39$	$-40 \le h \le 40$	$-14 \le h \le 14$	$-13 \le h \le 15$	$-35 \le h \le 35$
	$-39 \le k \le 42$	$-13 \le k \le 14$	$-15 \le k \le 15$	$-15 \le k \le 15$	$-10 \le k \le 11$
	$-28 \le l \le 20$	$-30 \le l \le 31$	$-20 \le l \le 20$	$-11 \le l \le 16$	$-17 \le l \le 17$
GOF (F^2)	1.003	0.981	1.063	0.911	1.034
R_1, wR_2 ($I > 2\sigma(I)$)	0.0475	0.0630	0.0534	0.0522	0.0304
	0.0989	0.1793	0.1674	0.0683	0.0750
R_1, wR_2 (all data)	0.0589	0.1159	0.0844	0.1127	0.0402
	0.1010	0.2047	0.1674	0.0765	0.0785

[a] $R_1 = \Sigma||F_o| - |F_c||/\Sigma|F_o|$. $wR_2 = [\Sigma w(F_o^2 - F_c^2)^2/\Sigma w(F_o^2)]^{1/2}$.

Table 2. Selected Bond Lengths (Å) and Angles (deg) for 1[a]

Cr1—C11	1.983(4)	Cr1—C12	2.033(4)
Cr1—C10	1.979(4)	Cr1—N5	2.035(3)
Cr1—N3	2.034(4)	Cr1—N1	2.018(4)
Cu1—N7#1	1.977(4)	Cu1—N7	1.977(4)
Cu1—N11#1	2.118(4)	Cu1—N11	2.118(4)
Cu1—N10	2.306(5)	Cu2—N8#1	1.976(4)
Cu2—N8	1.976(4)	Cu2—N12	2.110(4)
Cu2—N12#1	2.110(4)	Cu2—N13	2.150(6)
Cu3—N9#1	2.033(4)	Cu3—N9	2.033(4)
Cu3—N15#1	2.124(4)	Cu3—N15	2.124(4)
Cu3—N14	2.190(5)		
N7—C10—Cr1	173.80(3)	N8—C11—Cr1	169.80(4)
N9—C12—Cr1	171.30(4)	C11—Cr1—C12	90.70(2)
C12—Cr1—C10	93.08(2)	C10—Cr1—N5	89.66(2)
C12—Cr1—N3	89.32(2)	C10—N7—Cu1	172.50(4)
C11—N8—Cu2	175.30(4)	C12—N9—Cu3	172.50(3)
N7—Cu1—N10	100.73(2)	N11—Cu1—N10	83.21(1)
N7#2—Cu1—N7	85.90(2)	N7—Cu1—N11	95.42(2)
N8—Cu2—N13	106.30(2)	N12—Cu2—N13	83.29(2)
N12#3—Cu2—N12	82.40(2)	N8—Cu2—N12	94.42(2)
N9—Cu3—N14	104.06(1)	N15—Cu3—N14	83.53(1)
N9#2—Cu3—N15	96.19(1)	N15#2—Cu3—N15	82.20(2)

[a] Symmetry transformations used to generate equivalent atoms: #1 *x*, *x* − *y* + 1, *z*; #2 *x*, *x* − *y*, *z*; #3 *x*, *y* + 1, *z*.

trigonal bipyramidal geometry, bearing a C_3 axis and a 2-fold symmetry axis that passes through the Cu(1) center and bisects the Cu(3)−Cu(1)−Cu(2) angle, in which three square-pyramidal $[Cu(Me_3tacn)]^{2+}$ units are situated in the equatorial plane and two $[(Tp)Cr(CN)_3]^-$ units occupy the apical positions. Each Cr^{III} ion possesses a distorted octahedral coordination environment. The Cr^{III}−C(cyano) (2.018(4)−2.035(3) Å) and Cr^{III}−N(pyrazole) (1.979(4)−2.033(4) Å) bond lengths are within the normal values in the free tricyanometalate precursor, $[(Tp)Cr(CN)_3]^-$. Each Cu^{II} ion is coordinated to a Me_3tacn ligand as well as two nitrogen atoms of two cyanide bridges, forming a square-pyramidal coordination conformation. The basal positions of the square pyramid are occupied by two cyanide nitrogen atoms and two Me_3tacn nitrogen atoms with bond lengths of 1.976(4)−2.124(4) Å. The apical position is occupied by the remaining nitrogen atom of the Me_3tacn ligand with much longer bond lengths falling in the range 2.190(5)−2.306(5) Å. All cyanide bridges in the cluster deviate somewhat from linearity, as is reflected in the Cr−C≡N and Cu−N≡C angles (from 169.8(4)° to 175.3(4)°). The shortest intramolecular Cr···Cu, Cr···Cr, and Cu···Cu separations are 5.131, 6.393, and 6.603 Å, respectively, whereas the shortest intermolecular Cr···Cu, Cr···Cr, and Cu···Cu distances are 8.108, 8.942, and 8.782 Å, respectively. In **1**, there is a weak T-shaped C−H···*π* contact (3.665 Å) between the pyrazole ligands that results in formation of a three-dimensional (3D) network (Figure S2, Supporting Information).

dx.doi.org/10.1021/ic2011875 |*Inorg. Chem.* 2011, 50, 8636–8644

Table 3. Selected Bond Lengths (Å) and Angles (deg) for 2[a]

Cu1—O4	1.984(2)	Cu1— O1	1.995(3)
Cu1—N8	2.036(4)	Cu1—N9#1	2.048(5)
Cu1—O7	2.193(3)	Cr1—C12	1.972(3)
Cr1—C11	1.996(3)	Cr1—C10	2.028(5)
Cr1—N4	2.042(3)	Cr1—N6	2.043(3)
Cr1—N2	2.063(3)		
C11—N8—Cu1	175.60(4)	C12#1—N9#1—Cu1	176.40(4)
N8—C11—Cr1	175.90(3)	N9—C12—Cr1	176.80(4)
O4—Cu1—O1	87.80(11)	O4—Cu1—N8	168.37(14)
O1—Cu1—N8	88.74(13)	O4—Cu1—N9#1	87.15(12)
O1—Cu1—N9#1	163.05(14)	N8—Cu1—N9#1	93.00(14)
O4—Cu1—O7	91.89(11)	O1—Cu1—O7	92.87(11)
N8—Cu1—O7	99.37(14)	N9#1—Cu1—O7	103.45(14)

[a] Symmetry transformations used to generate equivalent atoms: #1 $-x$, $y + 2$, $-z$.

Table 4. Selected Bond Lengths (Å) and Angles (deg) for 3[a]

Cr1—N3	2.048(2)	Cr1—N1	2.059(2)
Cr1—C12	2.066(3)	Cr1—N5	2.0717(1)
Cr1—C10	2.072(2)	Cr1—C11	2.080(2)
Mn1—O1	2.132(2)	Mn1—O7	2.162(2)
Mn1—O4	2.178 (2)	Mn1—O10	2.220(2)
Mn1—N7	2.224(2)	Mn1—N8	2.240(2)
N7#1—C10—Cr1	174.40(2)	N8—C11—Cr1	171.70(2)
C10#1—N7—Mn1	171.70(2)	C11—N8—Mn1	172.40(2)
O7—Mn1—O10	175.68(7)	O1—Mn1—O7	90.83(7)
O1—Mn1—O4	85.53(7)	O7—Mn1—O4	88.18(7)
O1—Mn1—O10	93.32(8)		

[a] Symmetry transformations used to generate equivalent atoms: #1 $1 - x$, $1 - y$, $1 - z$.

Table 5. Selected Bond Lengths (Å) and Angles (deg) for 5[a]

C10—Cr1	2.099(1)	C11—Cr1	2.064(2)
C12—Cr1	2.067(2)	Cr1—N5	2.047(1)
Cr1—N3	2.051(1)	Cr1—N1	2.070(1)
Mn1—N8#1	2.211(1)	Mn1—N7	2.258(1)
Mn1—N10	2.305(1)	N7—C10—Cr1	175.88(1)
N8—C11—Cr1	176.15(1)	N9—C12—Cr1	171.98(1)
C10—N7—Mn1	155.21(1)	C11—N8—Mn1	156.20(1)
N5—Cr1—C12	87.89(6)	N3—Cr1—C12	87.93(6)
C11—Cr1—C12	91.53(6)	N5—Cr1—N1	87.96(5)
N3—Cr1—N1	85.19(5)	C11—Cr1—N1	92.43(6)
N8#1—Mn1—N10	96.45(5)	N8#2—Mn1—N10	82.98(5)
N7—Mn1—N10	90.22(4)	N10#3—Mn1—N10	71.18(6)
N8#1—Mn1—N7	87.98(5)	N8#2—Mn1—N7	92.42(5)

[a] Symmetry transformations used to generate equivalent atoms: #1 $1 - x$, $-y$, $-z$; #2 x, $-y$, $z - 1/2$; #3 $-x$, y, $-z$.

Complexes **2** and **3** show very similar structures, which contain neutral tetranuclear Cr_2M_2 clusters (M = Cu^{II} for **2** and Mn^{II} for **3**). Each M^{II} ion is linked to two $[(Tp)Cr(CN)_3]^-$ units at the cis positions, whereas each octahedral $[(Tp)Cr(CN)_3]^-$ unit uses its two cyanides to connect two M^{II} ions, leading to formation of the cyano-bridged rectangular cluster. As facial oxygen-containing tridentate ligand, the L_{OEt} fragments cap the M^{II} ions and

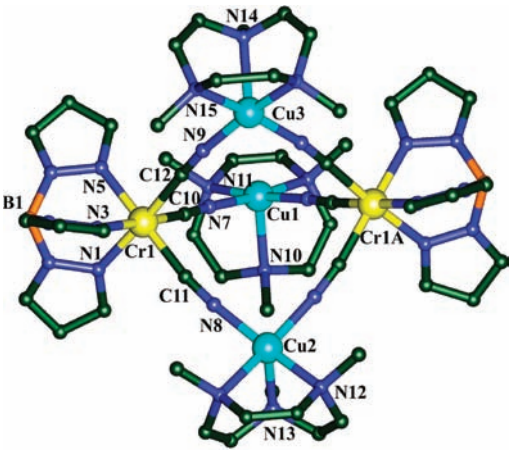

Figure 1. Perspective drawing of the pentanuclear cluster of complex **1** showing the atom numbering. H atoms are omitted for clarity.

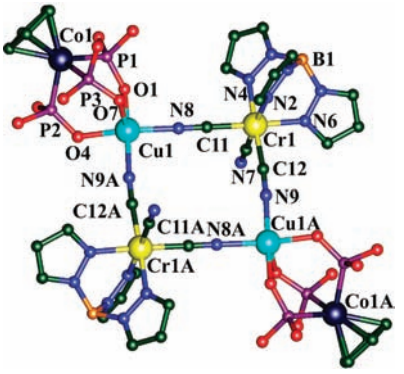

Figure 2. Perspective drawing of the tetranuclear cluster of complex **2** showing the atom numbering. Ethyl groups of the phosphates and H atoms are omitted for clarity.

connect the rectangle with trans modes and a crystallographic inversion center lies right in the center of the rectangle. The bond lengths and angles of the L_{OEt} and $[(Tp)Cr(CN)_3]^-$ moieties in both complexes are in good agreement with those in the related precursors.[22,5b] As shown in Figure 2, the Cu^{II} ions in **2** have a distorted square pyramidal coordination sphere, the equatorial plane is formed by two cyanide nitrogen atoms and two oxygen atoms of the L_{OEt} ligand with distances ranging from 1.984(2) to 2.048(5) Å, while the apical position is occupied by another oxygen atom of the tridentate L_{OEt} ligand with a longer distance of 2.199(3) Å. These bond lengths are somewhat longer than the related values in previously reported Fe_2Cu_2 bimetallic complex, $[(Tp)_2Fe_2(CN)_6Cu_2(L_{CoEt})_2]\cdot 6H_2O$.[22] The cyanide bridges connecting the metal centers are quite close to linearity with Cr−C≡N and Cu−N≡C angles from 175.6(4)° to 176.8(4)°. The intramolecular Cr···Cu distances are 5.148 and 5.153 Å; the Cr···Cr and Cu···Cu separations are 7.366 and 7.200 Å, respectively. The shortest intermolecular Cu···Cu, Cu···Cr, and Cr···Cr distances are 11.793, 8.734, and 8.154 Å, respectively. The adjacent clusters are connected through weak $\pi\cdots\pi$-stacking interactions between the pyrazole rings with centroid distances of 3.717 and 3.633 Å along the b and c direction, respectively, forming a 3D supramolecular framework (Figure S3, Supporting Information).

dx.doi.org/10.1021/ic2011875 |*Inorg. Chem.* 2011, 50, 8636–8644

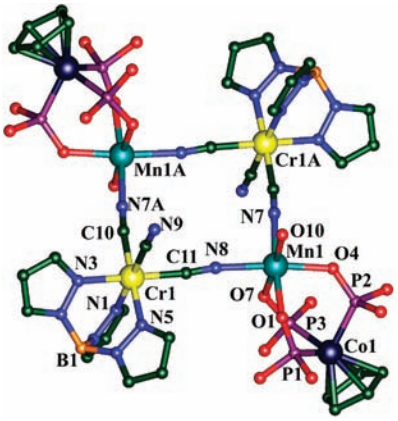

Figure 3. Perspective drawing of the tetranuclear cluster of complex **3** showing the atom numbering. Ethyl groups of the phosphates and H atoms are omitted for clarity.

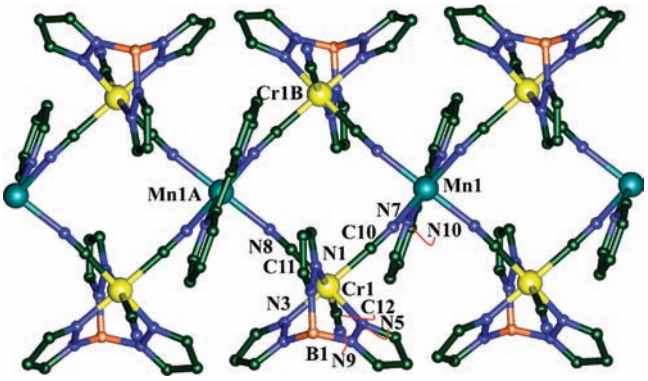

Figure 4. Perspective drawing of the 4,2-ribbon-like bimetallic chain of complex **5** showing the atom numbering. H atoms are omitted for clarity.

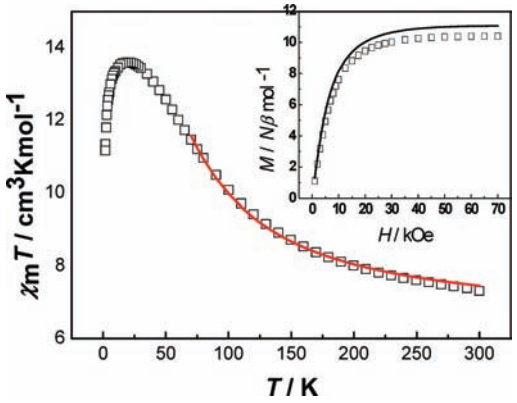

Figure 5. Temperature dependence of the $\chi_M T$ product for **1** at 2 kOe. (Inset) Field dependence of magnetization at 1.8 K. The lines represent the Brillouin function that corresponds to the $S = 9/2 + 3/2$ state (solid) with $g = 2.00$.

As shown in Figure 3, the Mn^{II} ions in complex **3** are hexacoordinated with N_3O_3 environments, showing a distorted octahedral geometry. The Mn−O_{LOEt} and Mn−N_{cyano} bond lengths are distributed in the range of 2.132(2)−2.240(2) Å (Table 3). The M−O_{MeOH} bond (2.220(2) Å) is somewhat longer than the M−O_{LOEt} bonds. The Cr−C≡N and Mn−N≡C angles vary from 171.7(2)° to 174.4(2)°, which are somewhat deviated from strict linearity. The shortest intramolecular $Cr^{III}\cdots Mn^{II}$, $Cr^{III}\cdots Cr^{III}$, and $Mn^{II}\cdots Mn^{II}$ separations are 5.422, 8.232, and 7.094 Å, respectively. The shortest intermolecular $Cr^{III}\cdots Mn^{II}$, $Cr^{III}\cdots Cr^{III}$, and $Mn^{II}\cdots Mn^{II}$ distances are 8.344, 7.816, and 10.097 Å, respectively. The adjacent clusters are connected through weak $\pi\cdots\pi$-stacking interactions between the pyrazole rings with centroid distances of 3.434 and 3.777 Å along the *ab* and *a* direction, respectively, forming the 3D supramolecular framework (Figure S4, Supporting Information).

Complex **4** consists of a cationic rectangular unit, $[(Tp)Cr(CN)_3Mn(phen)_2]_2^{2+}$, and two ClO_4^- anions. The $Cr_2^{III}Mn_2^{II}$ core is very similar to those of complexes **2** and **3**. As shown in Figure S5, Supporting Information, each $[(Tp)Cr(CN)_3]^-$ bridges two Mn^{II} ions in cis geometry and each Mn^{II} ion in turn links two $[(Tp)Cr(CN)_3]^-$ in a cis fashion as well. The manganese atom is hexacoordinated with two cyanide nitrogen atoms in cis positions and four nitrogen atoms from two phen ligands occupying the other sites, forming a slightly distorted octahedral surrounding. The Mn−N_{cyano} and Mn−N_{phen} bond lengths are in the range of 2.192(4)−2.193(3) and 2.239(4)−2.289(4) Å, respectively. The Mn−N_{cyano} bond lengths are somewhat shorter than those in complex **3** (2.224(2)−2.240(2) Å). The Mn−N≡C angles vary from 147.6(4)° to 156.0(4)°, which are more bent than those in complex **3** (171.6(4)−172.9(4)°). The intramolecular Cr···Mn, Mn···Mn, and Cr···Cr separations are 5.139, 6.380, and 8.212 Å, respectively. The shortest intermolecular $Cr^{III}\cdots Mn^{II}$, $Cr^{III}\cdots Cr^{III}$, and $Mn^{II}\cdots Mn^{II}$ distances are 8.414, 7.959, and 8.736 Å, respectively. The isolated square is connected through weak $\pi\cdots\pi$-stacking interactions between the phen rings, forming a 1D supramolecular chain (Figure S6, Supporting Information).

Compound **5** is made up of neutral cyano-bridged $Mn^{II}-Cr^{III}$ double zigzag chains. It is similar to $[M^{III}L(CN)_4]_2[M'^{II}(H_2O)_2]\cdot 4H_2O$ (L = phen, 2,2′-bpy; M = Fe, Cr; M′ = Mn, Co, Zn),[13a,23,24] which consist of 4,2-ribbon-like chains.[25] As shown in Figure 4, each $[(Tp)Cr(CN)_3]^-$ entity acts as a bidentate ligand toward the $[Mn(bpy)]^{2+}$ motifs through two of its three cyanide groups in cis positions, affording bimetallic double chains that run parallel to the *c* axis. These double chains show two orientations of their mean planes ($Cr^{III}_2Mn^{II}_2$) with a dihedral angle of 49°. The manganese atom is hexacoordinated with two nitrogen atoms from bpy in cis positions and four cyanide nitrogen atoms from four $[(Tp)Cr(CN)_3]^-$ units, forming a slightly distorted octahedral surrounding. The Mn−N_{cyano} bond lengths are in the range of 2.211(1)−2.258(1)°. The Mn−N≡C angles (155.21−156.20°) are more bent than Cr−C≡N angles (175.88−176.15°) for the bridging cyanides. The intramolecular Cr···Mn distances are 5.285 and 5.354 Å, and the Cr···Cr and Mn···Mn separations are 7.661 and 7.382 Å, respectively. The shortest interchain M···M distance is 8.117 Å. Each chain interacts with two other adjacent chains by $\pi\cdots\pi$ stacking between pyrazole rings with a centroid distance of 3.56 Å, thus forming the 3D structure (Figure S7, Supporting Information).

Magnetic Properties. The magnetic susceptibility variation at different temperatures of complex **1** (Cr_3Cu_3 unit) was measured at 1.8−300 K under 2 kOe (Figure 5). At 300 K, the $\chi_M T$ value of 7.00 $cm^3\cdot K\cdot mol^{-1}$ is close to 6.75 $cm^3\cdot K\cdot mol^{-1}$ expected for three Cr^{III} centers ($S = 3/2$) and three Cu^{II} centers ($S = 1/2$) assuming $g = 2.00$ and no exchange coupling. As the temperature

dx.doi.org/10.1021/ic2011875 |*Inorg. Chem.* 2011, 50, 8636–8644

decreases, the $\chi_M T$ values increase smoothly, reaching a maximum of 13.58 $cm^3 \cdot K \cdot mol^{-1}$ at 20 K. It indicates the presence of ferromagnetic exchange coupling between neighboring Cr^{III} and Cu^{II} ions. The magnetic susceptibility follows a Curie−Weiss law above 100 K with C = 6.08 $cm^3 \cdot K \cdot mol^{-1}$ and θ = 42.54 K, confirming the presence of dominant ferromagnetic interactions between neighboring Cr^{III} and Cu^{II} ions. Below 20 K, $\chi_M T$ drops down sharply, reaching 11.16 $cm^3 \cdot K \cdot mol^{-1}$ at 1.8 K, which could be attributed to the Zeeman effects associated with a high-spin ground state. The field dependence of magnetization was measured at 1.8 K (Figure 5, inset). There is a rapid increase from 0 to 25 kOe, and then it increases more slowly to a maximum value of 10.40 $N\beta$ at 70 kOe without reaching saturation, which further confirms the ferromagnetic interactions between neighboring Cr^{III} and Cu^{II} ions. The comparison between calculations based on the Brillouin function and the observed curves is shown in the inset of Figure 5. According to the structure, the exchange Hamiltonians of **1** can be described as $\hat{H} = -2J_1(\hat{S}_{Cr1}+\hat{S}_{Cr2})(\hat{S}_{Cu1}+\hat{S}_{Cu2}+\hat{S}_{Cu3}) - 2J_2(\hat{S}_{Cu1}\hat{S}_{Cu2}+\hat{S}_{Cu2}\hat{S}_{Cu3}+\hat{S}_{Cu3}\hat{S}_{Cu1}) - 2J_3\hat{S}_{Cr1}\hat{S}_{Cr2}$. The free anion with Cr(III) ion was included as a constant term ($\chi_M T = (Ng^2\beta^2/3k)S_{Cr2}(S_{Cr2}+1)$). Assuming $J_2 = J_3 = 0$, the best fitting results with a TIP correction were obtained from 70 to 300 K: g = 1.95; J_1 = 17.20 cm^{-1}; zJ' = 0.20 cm^{-1}; TIP = 0.0005 emu mol^{-1} ($R = 6.25 \times 10^{-3}$), which are comparable with those in $[(Me_3tacn)_5Cu_3Cr_2(CN)_6](ClO_4)_6 \cdot 5CH_3CN$.[21] For **1**, the J value is much higher than the related value in the Fe_2Cu_3 cluster,[12a] which also confirms that substituting Cr^{III} for Fe^{III} is an effective means of increasing the strength of the magnetic exchange coupling.

To probe the ground state of the cluster of **1**, field-dependent magnetization data were collected in the temperature range of 1.8−10 K (Figure S8, Supporting Information). The superposition of the lines in different magnetic fields is observed, suggesting inexistence of zero-field splitting in complex **1**. Alternating current magnetic susceptibility measurements were also performed at various switching frequencies, and there is no signal in the out-of-phase magnetic susceptibility (Figure S9, Supporting Information). Compared with the Fe_2Cu_3 cluster,[12a] which shows single-molecule magnet behavior, complex **1** is obviously not a SMM. Although the Cu^{2+} ions exhibit single-ion anisotropy due to a first-order Jahn−Teller distortion, the Cr^{3+} ions possess completely quenched first-order orbital angular momentum due to a fully symmetric ($^4A_{2g}$) ground term,[21] which has no anisotropy in the axial positions. Thus, it suggests that the single-ion anisotropy from the axial positions plays the most significant role in controlling the overall molecular anisotropy.

Since the Co^{III} ion is diamagnetic, the magnetic properties of complexes **2** and **3** can be regarded as analogies of cyano-bridged $Cr^{III}{}_2M^{II}{}_2$ (M = Cu^{II} for **2**; Mn^{II} for **3**) molecular squares.

The $\chi_M T$ versus T plot of **2** is shown in Figure 6. The value per $[Cu_2Cr_2]$ at 300 K is 5.43 $cm^3 \cdot K \cdot mol^{-1}$, which is much higher than the expected value of 4.50 $cm^3 \cdot K \cdot mol^{-1}$ for two isolated Cu^{II} ions (S = 1/2) and two Cr^{III} ions (S = 3/2) in the spin-only approach. $\chi_M T$ increases smoothly from room temperature to reach a maximum value of 10.05 $cm^3 \cdot K \cdot mol^{-1}$ at 18 K and then decreases sharply, reaching 8.02 $cm^3 \cdot K \cdot mol^{-1}$ at 1.8 K. This is consistent with the behavior expected for intramolecular ferromagnetic interactions between Cu^{II} and Cr^{III} ions. The magnetic susceptibility of **2** follows a Curie−Weiss law above 150 K with a Curie constant C = 4.61 $cm^3 \cdot K \cdot mol^{-1}$ and a Weiss constant θ = 51.84 K. The C value is very similar to the expected one (4.50 $cm^3 \cdot K \cdot mol^{-1}$ for g = 2.00) for two noninteracting Cr^{III} ions and two noninteracting Cu^{II} ions. The positive sign of θ indicates the presence of dominant ferromagnetic interactions between neighboring Cr^{III} and Cu^{II} ions. The field dependence of the magnetization (0−70 kOe) measured at 1.8 K is shown in Figure 6(inset) in the form of $M/N\beta$ versus H. The magnetization tends to 8.16 $N\beta$, which is close to the expected value for two Cu^{II} ions and two Cr^{III} ions system (S = 4). The magnetization values are fitted well with the Brillouin curve corresponding to S = 4 and higher than the Brillouin curve for noninteracting $S = 2S_{Cr} + 2S_{Cu}$ with g = 2.00, confirming the overall ferromagnetic Cr^{III}−Cu^{II} interaction. On the basis of the structure, the Hamiltonian of **2** can be described as the following: $\hat{H} = -2J\hat{S}_{Cr1}(\hat{S}_{Cu1}+\hat{S}_{Cu2}) - 2J\hat{S}_{Cr2}(\hat{S}_{Cu1}+\hat{S}_{Cu2})$, which includes only nearest-neighbor exchange. The best fit between 1.8 and 300 K gave g = 2.04, J = 25.3 cm^{-1}, and zJ' = −0.03 cm^{-1}. The J value is very large and comparable with the related values in the zigzag chain compound $(Bu_4N)[TpCuReCl_4(CN)_2]$ and the heptanuclear cluster $[(tren)_6Cu_6Cr(CN)_6]^{9+}$ (tren = tris(2-amino)-ethylamine).[26,2d] Such strong magnetic coupling arises from the presence of a d^3 electron configuration with local C_{3v} symmetry. The square pyramidal coordination of the Cu^{II} center lowers the energy of the $d_z{}^2$ orbital, thereby localizing the unpaired electron along the Cu−N_{CN} bond in the direction of magnetic exchange.[26]

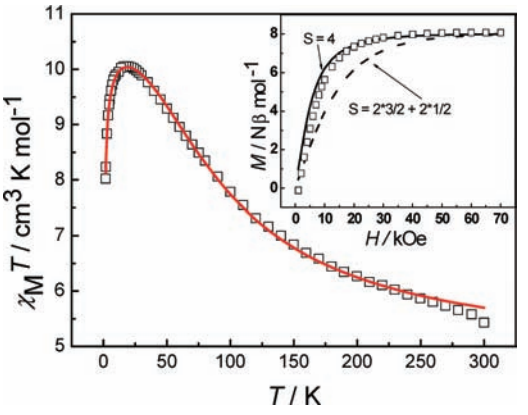

Figure 6. Temperature dependence of the $\chi_M T$ product for **2** at 2 kOe. (Inset) Field dependence of magnetization at 1.8 K. The lines represent the Brillouin function that corresponds to the S = 4 state (solid) and noninteracting $S = 2S_{Cr}{}^{III} + 2S_{Cu}{}^{II}$ (break) with g = 2.00.

The temperature dependence of susceptibility under 2 kOe for complexes **3** and **4** is displayed in Figures 7 and S10, Supporting Information. The $\chi_M T$ value at 300 K is 10.84 $cm^3 \cdot K \cdot mol^{-1}$ for **3**, which is smaller than the expected value of 13.50 $cm^3 \cdot K \cdot mol^{-1}$ for two spin-isolated Cr^{III} (S = 3/2) and two high-spin Mn^{II} (S = 5/2) ions in the absence of any exchange coupling. For **4**, the $\chi_M T$ value at 300 K is 13.19 $cm^3 \cdot K \cdot mol^{-1}$, close to the expected value of 13.50 $cm^3 \cdot K \cdot mol^{-1}$. As the temperature is lowered, the $\chi_M T$ values decrease gradually and reach a plateau at ∼10 K for **3** and **4**, suggesting the presence of significant antiferromagnetic interaction between neighboring Mn^{II} and Cr^{III} ions. Then they decrease abruptly at ∼3 K, reaching 2.55 $cm^3 \cdot K \cdot mol^{-1}$ for **3** at 1.8 K and 3.75 $cm^3 \cdot K \cdot mol^{-1}$ for **4** at 2.0 K, which may be due to intercluster antiferromagnetic coupling and/or ZFS and/or magnetic saturation effects. The field-dependent magnetization measurements (insert of Figure 7 and Figure S9, Supporting Information) gives the value of 3.95 $N\beta$ at 70 kOe for **3** and 4.04 $N\beta$ at 50 kOe for **4**, which are consistent with the expected

dx.doi.org/10.1021/ic2011875 |Inorg. Chem. 2011, 50, 8636–8644

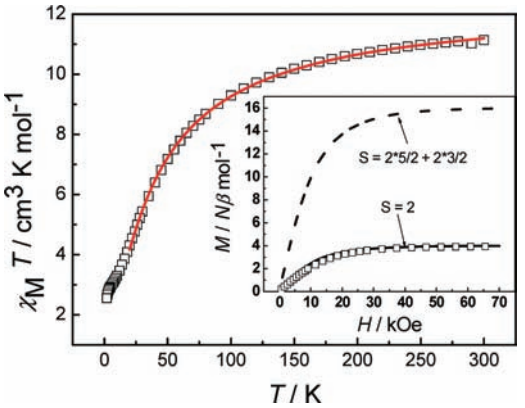

Figure 7. Temperature dependence of the $\chi_M T$ product for **3** at 2 kOe. Solid lines represent the best fits of the data. (Inset) Field dependence of magnetization at 1.8 K. The lines represent the Brillouin function that corresponds to the $S = 2$ state (solid) and noninteracting $S = 2S_{Cr}^{III} + 2S_{Mn}^{II}$ (break) with $g = 2.00$.

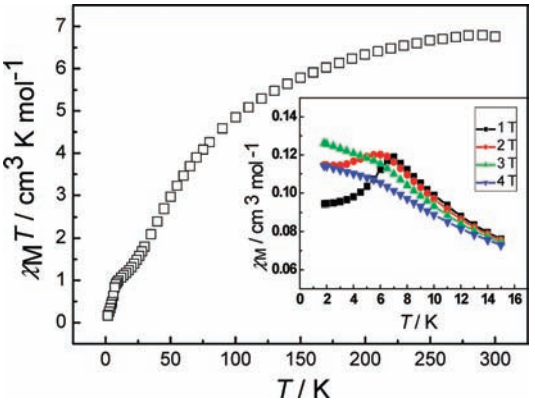

Figure 8. Temperature dependence of the $\chi_M T$ product for **5** at 2 kOe. (Inset) Thermal dependence of the magnetic susceptibility at $T \leq 16$ K.

value for the antiferromagnetic state of Mn_2Cr_2 cluster. The comparison between calculations based on the Brillouin function and the observed curves is also shown in the inset of Figure 7 for **3** and Figure S9, Supporting Information, for **4**.

On the basis of the crystal structures of compound **3**, we can assume that there is only one exchange mode ($Mn^{II}-CN-Cr^{III}$). Thus, the appropriate Hamiltonian would be $\hat{H} = -2J\hat{S}_{Cr1}(\hat{S}_{Mn1} + \hat{S}_{Mn2}) - 2J\hat{S}_{Cr2}(\hat{S}_{Mn1} + \hat{S}_{Mn2})$, in which J is the coupling constant through the cyano bridges. By means of Kambe's method, the data are fitted and the corresponding results are obtained: $g = 1.99$, $J = -2.05$ cm^{-1} and $zj' = -0.47$ cm^{-1} ($R = 2.18 \times 10^{-3}$), indicating the existence of antiferromagnetic interaction between Mn^{II} and Cr^{III} ions. Compared with the related value in previously reported Fe_2Mn_2 cluster,[22] the absolute value of J is somewhat higher. Arising from the π-donating ability, the presence of L_{OEt} in compounds **2** and **3** may account for the magnetic properties, although it is difficult to give a detailed and quantitative explanation. For compound **4**, the Mn−N≡C angles of the cyano bridges are distinctly different (147.6(4)° and 156.0(4)°) and there is no suitable theoretical model to analyze the magnetic data, which precludes determination of the values of the intramolecular magnetic interactions between Cr^{III} and Mn^{II} ions.

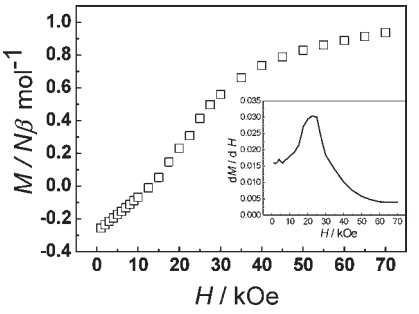

Figure 9. Field dependence of magnetization at 1.8 K for **5**. (Insert) dM/dH vs H plot.

The susceptibility variation at different temperature of complex **5** ($MnCr_2$ unit) was measured under 2 kOe at 1.8−300 K (Figure 8). The $\chi_M T$ value at 300 K is 6.76 cm^3·K·mol^{-1}, which is much lower than the value calculated for two magnetically isolated spin quartets Cr(III) and one spin sextet Mn(II) (8.13 cm^3·K·mol^{-1} with $g = 2.00$). It continuously decreases upon cooling and then tends to a plateau with 1.31 cm^3·K·mol^{-1} at 20 K, indicating the presence of intrachain antiferromagnetic coupling between neighboring Cr^{III} and Mn^{II} ions. It decreases at lower temperatures to reach 0.16 cm^3·K·mol^{-1} at 1.8 K, which may be ascribed to interchain antiferromagnetic interactions. Evaluation of the intrachain antiferromagnetic interactions in **5** is precluded by the lack of a suitable model to analyze the magnetic data. The magnetic susceptibility of **5** is field dependent at very low temperature (inset of Figure 8). A maximum of χ_M was observed at 7 K under 1 T, indicating antiferromagnetism of **5** under this condition. The maximum broadens and shifts to lower temperature as the magnetic field increases, and it finally disappears for $H \geq 3$ T. This behavior shows the existence of a field-induced magnetic phase transition. The sigmoid shape of the magnetization (M) versus field (H) plot further confirms the metamagnetic behavior of **5** (Figure 9). The comparison between calculations based on the Brillouin function and the observed curves is also shown in the inset of Figure S11, Supporting Information. From the variable-temperature magnetization measurements at different low fields and dM/dH vs H plot at 1.8 K (insert of Figure 9) the critical field is estimated to be about 22.5 kOe. A similar magnetic behavior has been reported previously in the neutral cyano-bridged chain complex, $[Cr(ampy)(CN)_4]_2Mn(H_2O)_4 \cdot 6H_2O$.[27]

CONCLUSIONS

In summary, using $[(Tp)Cr(CN)_3]^-$ as the building block, a trigonal bipyramidal $Cr^{III}{}_2Cu^{II}{}_3$ (**1**) cluster, three tetranuclear rectangular $Cr^{III}{}_2M^{II}{}_2$ (M = Cu for **2**, Mn for **3** and **4**) clusters, and a 4,2-ribbon-like chain (**5**) were synthesized and structurally characterized. Their magnetic properties have been studied. As expected, no SMM behavior is observed for all cluster complexes (**1**−**4**), confirming that the single-ion anisotropy from the axial positions is the key to the molecular anisotropy. Complex **5** behaves as metamagnet with a H_c value of 22.5 kOe at 1.8 K. For complexes **1** and **2**, the Cu−Cr coupling constants (J) are obviously much higher than those in the related Cu−Fe cluster. The results confirm that the use of Cr^{III} ion is an effective means of increasing the strength of the magnetic exchange coupling and is useful for new molecular magnetic materials.

dx.doi.org/10.1021/ic2011875 |Inorg. Chem. 2011, 50, 8636–8644

■ ASSOCIATED CONTENT

Supporting Information. Additional structure and magnetic characterization data, and X-ray crystallographic files in CIF format for **1**−**5**. This material is available free of charge via the Internet at http://pubs.acs.org.

■ AUTHOR INFORMATION

Corresponding Author
*Fax: +86-25-83314502. E-mail: zuojl@nju.edu.cn.

■ ACKNOWLEDGMENT

This work was supported by the Major State Basic Research Development Program (2007CB925100 and 2011CB808704), the National Science Fund for Distinguished Young Scholars of China (20725104), and the National Natural Science Foundation of China (21021062 and 91022031). We also thank Prof. Yi-Zhi Li for structure refinements and Prof. You Song and Dr. Tian-Wei Wang for helpful discussions and experimental assistance on magnetic measurements.

■ REFERENCES

(1) (a) Barrar, A. L.; Debrunner, P.; Gatteschi, D.; Schulz, C. E.; Sessoli, R. *Europhys. Lett.* **1996**, *35*, 133. (b) Castro, S. L.; Sun, Z.; Grant, C. M.; Bollinger, J. C.; Hendrickson, D. N.; Christou, G. *J. Am. Chem. Soc.* **1998**, *120*, 2365. (c) Barrar, A. L.; Caneschi, A.; Cornia, A.; Fabrizi, B. F.; Gatteschi, D.; Sangregorio, C.; Sessoli, R.; Sorace, L. *J. Am. Chem. Soc.* **1999**, *121*, 5302. (d) Boskovic, C.; Pink, M.; Huffman, J. C.; Hendrickson, D. N.; Christou, G. *J. Am. Chem. Soc.* **2001**, *123*, 9914. (e) Boskovic, C.; Brechin, E. K.; Streib, W. E.; Folting, K.; Bollinger, J. C.; Hendrickson, D. N.; Christou, G. *J. Am. Chem. Soc.* **2002**, *124*, 3725. (f) Tasiopoulos, A. J.; Wernsdorfer, W.; Moulton, B.; Zaworotko, M. J.; Christou, G. *J. Am. Chem. Soc.* **2003**, *125*, 15274. (g) Oshio, H.; Hoshino, N.; Ito, T.; Nakano, M. *J. Am. Chem. Soc.* **2004**, *126*, 8805. (h) Maheswaran, S.; Chastanet, G.; Teat, S. J.; Mallah, T.; Sessoli, R.; Wernsdorfer, W.; Winpenny, R. E. P. *Angew. Chem., Int. Ed.* **2005**, *44*, 5044. (i) Zeng, M. H.; Yao, M. X.; Liang, H.; Zhang, W. X.; Chen, X. M. *Angew. Chem., Int. Ed.* **2007**, *46*, 1832. (j) Guo, Y. N.; Xu, G. F.; Gamez, P.; Zhao, L.; L; Lin, S. Y.; Deng, R. P.; Tang, J. K.; Zhang, H. J. *J. Am. Chem. Soc.* **2010**, *132*, 8538.

(2) (a) Dunbar, K. R.; Heintz, R. A. *Prog. Inorg. Chem.* **1997**, *45*, 283. (b) Weihe, H.; Güdel, H. U. *Comments Inorg. Chem.* **2000**, *22*, 75. (c) Miller, J. S. *MRS Bull.* **2000**, *25*, 60. (d) Marvaud, V.; Decroix, C.; Scuiller, A.; Guyard Duhayon, C.; Vaissermann, J.; Gonnet, F.; Verdaguer, M. *Chem.—Eur. J.* **2003**, *9*, 1677. (e) Marvaud, V.; Decroix, C.; Scuiller, A.; Tuyéras, F.; Guyard-Duhayon, C.; Vaissermann, J.; Marrot, J.; Gonnet, F.; Verdaguer, M. *Chem.—Eur. J.* **2003**, *9*, 1692. (f) Wang, S.; Zuo, J. L.; Zhou, H. C.; Choi, H. J.; Ke, Y. X.; Long, J. F.; You, X. Z. *Angew. Chem., Int. Ed.* **2004**, *43*, 5940. (g) Beltran, L. M. C.; Long, J. R. *Acc. Chem. Res.* **2005**, *38*, 325 and references therein..

(3) (a) Arimoto, Y.; Ohkoshi, S. I.; Zhong, Z. J.; Seino, H.; Mizobe, Y.; Hashimoto, K. *J. Am. Chem. Soc.* **2003**, *125*, 9240. (b) Sato, O. *Acc. Chem. Res.* **2003**, *36*, 692. (c) Niel, V.; Thompson, A. L.; Muñnoz, M. C.; Galet, A.; Goeta, A. E.; Real, J. A. *Angew. Chem., Int. Ed.* **2003**, *42*, 3760. (d) Nihei, M.; Ui, M.; Yokota, M.; Han, L.; Maeda, A.; Kishida, H.; Okamoto, H.; Oshio, H. *Angew. Chem., Int. Ed.* **2005**, *44*, 6484. (e) Shatruk, M.; Dragulescu-Andrasi, A.; Chambers, K. E.; Stoian, S. A.; Bominaar, E. L.; Achim, C.; Dunbar, K. R. *J. Am. Chem. Soc.* **2007**, *129*, 6104. (f) Li, D. F.; Clérac, R.; Roubeau, O.; Harté, E.; Mathonière, C.; Le Bris, R.; Holmes, S. M. *J. Am. Chem. Soc.* **2008**, *130*, 7656. (g) Song, Y.; Zhang, P.; Ren, X. M.; Shen, X. F.; Li, Y. Z.; You, X. Z. *J. Am. Chem. Soc.* **2005**, *127*, 3708. (h) Li, D. F.; Parkin, S.; Wang, G. B.; Yee, G. T.; Clérac, R.; Wernsdorfer, W.; Holmes, S. M. *J. Am. Chem. Soc.* **2006**, *128*, 4214. (i) Freedman, D. E.; Jenkins, D. M.; Iavarone, A. T.; Long, J. R. *J. Am. Chem. Soc.* **2008**, *130*, 2884. (j) Lescouëzec, R.; Vaissermann, J.; Ruiz-Pérez, C.; Lloret, F.; Carrasco, R.; Julve, M.; Verdaguer, M.; Dromzee, Y.; Gatteschi, D.; Wernsdorfer, W. *Angew. Chem., Int. Ed.* **2003**, *42*, 1483. (k) Harris, T. D.; Bennett, M. V.; Clérac, R.; Long, J. R. *J. Am. Chem. Soc.* **2010**, *132*, 3980. (l) Zhang, Y. Z.; Li, D. F.; Clérac, R; Kalise, M.; Mathonière, C.; Holmes., S. M. *Angew. Chem., Int. Ed.* **2010**, *49*, 3752. (m) Nihei, M.; Sekine, Y.; Suganami, N.; Nakazawa, K.; Nakao, A.; Nakao, H.; Murakami, Y.; Oshio, H. *J. Am. Chem. Soc.* **2011**, *133*, 3592.

(4) Li, D. F.; Parkin, S.; Wang, G. B.; Yee, G. T.; Holmes, S. M. *Inorg. Chem.* **2006**, *45*, 2773.

(5) (a) Sokol, J. J.; Shores, M. P.; Long, J. R. *Angew. Chem., Int. Ed.* **2001**, *40*, 236. (b) Harris, T. D.; Long, J. R. *Chem. Commun.* **2007**, 1360. (c) Yang, J. Y.; Shores, M. P.; Sokol, J. J.; Long, J. R. *Inorg. Chem.* **2003**, *42*, 1403. (d) Li, D. F.; Ruschman, C.; Parkin, S.; Clérac, R.; Holmes, S. M. *Chem. Commun.* **2006**, 4036.

(6) (a) Li, D. F.; Parkin, S.; Wang, G.; Yee, G. T.; Prosvirin, A. V.; Holmes, S. M. *Inorg. Chem.* **2005**, *44*, 4903. (b) Li, D. F.; Clérac, R.; Parkin, S.; Wang, G. B.; Yee, G. T.; Holmes, S. M. *Inorg. Chem.* **2006**, *45*, 5251. (c) Jiang, L.; Feng, X. L.; Lu, T. B.; Gao, S. *Inorg. Chem.* **2006**, *45*, 5018. (d) Ni, Z. H.; Kou, H. Z.; Zhang, L. F.; Ni, W. W.; Jiang, Y. B.; Cui, A. L.; Ribas, J.; Sato, O. *Inorg. Chem.* **2005**, *44*, 9631. (e) Ni, Z. H.; Kou, H. Z.; Zhao, Y. H.; Zheng, L.; Wang, R. J.; Cui, A. L.; Sato, O. *Inorg. Chem.* **2005**, *44*, 2050. (f) Ni, W. W.; Ni, Z. H.; Cui, A. L.; Liang, X.; Kou, H. Z. *Inorg. Chem.* **2007**, *46*, 22. (g) Kim, J.; Han, S.; Pokhodnya, K. I.; Migliori, J. M.; Miller, J. S. *Inorg. Chem.* **2005**, *44*, 6983. (h) Jiang, L.; Choi, H. J.; Feng, X. L.; Lu, T. B.; Long, J. R. *Inorg. Chem.* **2007**, *46*, 2181. (i) Nihei, M.; Ui, M.; Hoshino, N.; Oshio, H. *Inorg. Chem.* **2008**, *47*, 6106. (j) Zhang, Y. J.; Liu, T.; Kanegawa, S.; Sato, O. *J. Am. Chem. Soc.* **2009**, *131*, 7942. (k) Kim, J. I.; Yoo, H. S.; Koh, E. K.; Hong, C. S. *Inorg. Chem.* **2007**, *46*, 10461. (l) Kwak, H. Y.; Ryu, D. W.; Lee, J. W.; Yoon, J. H.; Kim, H. C.; Koh, E. K.; Krinsky, J.; Hong, C. S. *Inorg. Chem.* **2010**, *49*, 4632. (m) Xiang, J.; Man, W. L.; Guo, J. F.; Yiu, S. M.; Lee, G. H.; Peng, S. M.; Xu, G. C.; Gao, S.; Lau, T. C. *Chem. Commun.* **2010**, 6102. (n) Zhang, Y. Z.; Wang, Z. M.; Gao, S. *Inorg. Chem.* **2006**, *45*, 5447.

(7) (a) Shores, M. P.; Sokol, J. J.; Long, J. R. *J. Am. Chem. Soc.* **2002**, *124*, 2279. (b) Rebilly, J. N.; Catala, L.; Charron, G.; Rogez, G.; Rivière, E.; Guillot, R.; Thuéry, P.; Barra, A. L.; Mallah, T. *Dalton Trans.* **2006**, 2818. (c) Rebilly, J. N.; Catala, L.; Rivière, E.; Guillot, R.; Wernsdorfer, W.; Mallah, T. *Inorg. Chem.* **2005**, *44*, 8194.

(8) (a) Yoon, J. H.; Lim, J. H.; Kim, H. C.; Hong, C. S. *Inorg. Chem.* **2006**, *45*, 9613. (b) Choi, S. W.; Kwak, H. Y.; Yoon, J. H.; Kim, H. C.; Koh, E. K.; Hong, C. S. *Inorg. Chem.* **2008**, *47*, 10214.

(9) (a) Schelter, E. J.; Bera, J. K.; Bacsa, J.; Galn-Mascars, J. R.; Dunbar, K. R. *Inorg. Chem.* **2003**, *42*, 4256. (b) Schelter, E. J.; Prosvirin, A. V.; Dunbar, K. R. *J. Am. Chem. Soc.* **2004**, *126*, 15004. (c) Schelter, E. J.; Prosvirin, A. V.; Reiff, W. M.; Dunbar, K. R. *Angew. Chem., Int. Ed.* **2004**, *43*, 4912. (d) Schelter, E. J.; Karadas, F.; Avendano, C.; Prosvirin, A. V.; Wernsdorfer, W.; Dunbar., K. R. *J. Am. Chem. Soc.* **2007**, *129*, 8139. (e) Karadas, F.; Schelter, E. J.; Shatruk, M.; Prosvirin, A. V.; Bacsa, J.; Smirnov, D.; Ozarowski, A.; Krzystek, J.; Telser, J.; Dunbar, K. R. *Inorg. Chem.* **2008**, *47*, 2074.

(10) (a) Palii, A.; Ostrovsky, S. M.; Klokishner, S. I.; Tsukerblat, B. S.; Dunbar, K. R. *ChemPhysChem* **2006**, *7*, 871. (b) Park, K.; Holmes, S. M. *Phys. Rev. B* **2006**, *74*, 224440. (c) Wang, C. F.; Liu, W.; Song, Y.; Zhou, X. H.; Zuo, J. L.; You, X. Z. *Eur. J. Inorg. Chem.* **2008**, 717.

(11) (a) Wang, S.; Zuo, J. L.; Zhou, H. C.; Song, Y.; Gao, S.; You, X. Z. *Eur. J. Inorg. Chem.* **2004**, 3681. (b) Gu, Z. G.; Yang, Q. F.; Liu, W.; Song, Y.; Li, Y. Z.; Zuo, J. L.; You, X. Z. *Inorg. Chem.* **2006**, *45*, 8895.

(12) (a) Wang, C. F.; Zuo, J. L.; Bartlett, B. M.; Song, Y.; Long, J. R.; You, X. Z. *J. Am. Chem. Soc.* **2006**, *128*, 7162. (b) Liu, W.; Wang, C. F.; Li, Y. Z.; Zuo, J. L.; You, X. Z. *Inorg. Chem.* **2006**, *45*, 10058. (c) Gu, Z. G.; Liu, W.; Yang, Q. F.; Zhou, X. H.; Zuo, J. L.; You, X. Z. *Inorg. Chem.* **2007**, *46*, 3236.

(13) (a) Wang, S.; Zuo, J. L.; Gao, S.; Song, Y.; Zhou, H. C.; Zhang, Y. Z.; You, X. Z. *J. Am. Chem. Soc.* **2004**, *126*, 8900. (b) Wen, H. R.; Wang, C. F.; Song, Y.; Gao, S.; Zuo, J. L.; You, X. Z. *Inorg. Chem.* **2006**, *45*, 8942.

(14) (a) Lescouëzec, R.; Lloret, F.; Julve, M.; Vaissermann, J.; Verdaguer, M.; Llusar, R.; Uriel, S. *Inorg. Chem.* **2001**, *40*, 2065. (b) Toma, L.; Lescouëzec, R.; Vaissermann, J.; Delgado, F. S.; Ruiz-Pérez, C.; Carrasco, R.; Cano, J.; Lloret, F.; Julve, M. *Chem.—Eur. J.* **2004**, *10*, 6130.

(15) Zhang, Y. Z.; Gao, S.; Sun, H. L.; Su, G.; Wang, Z. M.; Zhang, S. W. *Chem. Commun.* **2004**, 1906.

(16) Burdett, J. K. *Molecular shapes-Theoretical Models of Inorganic Stereochemistry*; Wiley: New York, 1980; Chapters 9 and 12.

(17) (a) Kläui, W.; Muller, A.; Eberspach, W.; Boese, R.; Goldbergs, I. *J. Am. Chem. Soc.* **1987**, *109*, 164. (b) Kläui, W. *Angew. Chem., Int. Ed.* **1990**, *29*, 627 and references therein..

(18) *SAINT-Plus*, version 6.02; Bruker Analytical X-ray System: Madison, WI, 1999.

(19) Sheldrick, G. M. *SADABS: An Empirical Absorption Correction Program*; Bruker Analytical X-ray Systems: Madison, WI, 1996.

(20) Sheldrick, G. M. *SHELXTL-97*; Universität of Göttingen: Göttingen, Germany, 1997.

(21) Bartlett, B. M.; Harris, T. D.; DeGroot, M. W.; Long, J. R. *Z. Anorg. Allg. Chem.* **2007**, *633*, 2380.

(22) Kang, L. C.; Yao, M. X.; Chen, X.; Li, Y. Z.; Song, Y.; Zuo, J. L.; You, X. Z. *Dalton. Trans.* **2011**, 2204.

(23) (a) Lescouëzec, R.; Vaissermann, J.; Ruiz-Pérez, C.; Lloret, F.; Carrasco, R.; Julve, M.; Verdaguer, M.; Dromzee, Y.; Gatteschi, D.; Wernsdorfer, W. *Angew. Chem., Int. Ed.* **2003**, *42*, 1483. (b) Toma, L. M.; Lescouëzec, R.; Lloret, F.; Julve, M.; Vaissermann, J.; Verdaguer, M. *Chem. Commun.* **2003**, 1850. (c) Lescouëzec, R.; Lloret, F.; Julve, M.; Vaissermann, J.; Verdaguer, M.; Llusar, R.; Uriel, S. *Inorg. Chem.* **2001**, *40*, 2065. (d) Toma, L.; Lescouëzec, R.; Vaissermann, J.; Delgado, F. S.; Ruiz-Pérez, C.; Carrasco, R.; Cano, J.; Lloret, F.; Julve, M. *Chem.—Eur. J.* **2004**, *10*, 6130.

(24) Zhang, Y. Z.; Gao, S.; Wang, Z. M.; Su, G.; Sun, H. L.; Pan, F. *Inorg. Chem.* **2005**, *44*, 4534.

(25) Černák, J.; Orendáč, M.; Potočňák, I.; Chomič, J.; Orendáčová, A.; Skoršepa, J.; Feher, A. *Coord. Chem. Rev.* **2002**, *224*, 51 and references therein.

(26) Harris, T. D.; Coulon, C.; Clérac, R.; Long, J. R. *J. Am. Chem. Soc.* **2011**, *133*, 123.

(27) Toma, L.; Lescouëzec, R.; Vaissermann, J.; Herson, P.; Marvaud, V.; Lloret, F.; Julve, M. *New J. Chem.* **2005**, *29*, 210.